

# Literature review of humanoid robotic systems

12 June 2019

# Table of contents

|   |           |
|---|-----------|
| <b>Hand mechanisms</b>  | <b>3</b>  |
| A Multigrasp Hand Prosthesis for Providing Precision and Conformal Grasps.                            | 4         |
| Design of a multigrasp transradial prosthesis.  | 8         |
| <b>Wrist mechanisms</b>   | <b>12</b> |
| Kinematic Optimization of a Novel Partially Decoupled Three Degree of Freedom Hybrid Wrist Mechanism. | 13        |
| <b>Lower-limb mechanisms</b>  | <b>15</b> |
| Biomechanical Considerations in the Design of Lower Limb Exoskeletons.                                | 16        |
| Passive-dynamic leg design for agile robots.  | 18        |
| Design of a quasi-passive knee exoskeleton to assist running.   | 21        |
| <b>Walking theory</b>   | <b>25</b> |
| Compliant leg behavior explains basic dynamics of walking and running.                                | 26        |
| <b>Walking control techniques</b>   | <b>31</b> |
| Actuated Dynamic Walking in a Seven-Link Biped Robot.   | 32        |
| A Control Approach for Actuated Dynamic Walking in Biped Robots.                                      | 34        |
| <b>Walking robots</b>   | <b>36</b> |
| Walking and Running with Passive Compliance.  | 37        |
| <b>Performance metrics</b>  | <b>41</b> |
| (coming soon)   |           |

# Hand mechanisms

## A multigrasp hand prosthesis for providing precision and conformal grasps 2014

Daniel Bennett, Skylar Dalley, Don Truex, Michael Goldfarb.

- Goal:
  - Present a 16 DOF hand prosthesis, actuated by 4 motors, that can perform a variety of grasps
- Background:
  - Grasps can be classified as either *precision* or *conformal*
    - Precision grasps:
      - Tip, tripod, and lateral pinch grasps
      - Meant to provide dexterity
      - Single point of contact between object and each digit
    - Conformal grasps:
      - Hook, spherical, and cylindrical grasps
      - Meant to provide stability
      - Multiple points of contact between fingers and object
  - The 6 grasps described above constitute the vast majority of the grasps used by healthy individuals during the activities of daily living [15, 16]
    - In addition, the pointing and platform hand positions are helpful [17]
  - Digit forces and speeds: [18 - 20]
    - Digits associated with precision grasps (thumb and forefinger) should be capable of up to 25 N each
    - Digits for conformal grasps should be capable of up to 14 N total
    - All digits should be capable of 1.5 Hz over half their range of motion
  - Physical specifications: [21 - 24]
    - Hand should weigh around 500 g
    - A 50% male hand has a width of 9 cm and a length of 19.3 cm [26]
- Related work:
  - See related work section of document 2 in this folder
- Implementation:
  - See figure 1 and figure 2
  - Four motors:
    - Thumb (palmar ab/adduction), bidirectional tendon actuation
    - Thumb (flexion/extension), bidirectional tendon actuation
      - PIP joints are fused
    - Pointer finger (flexion/extension), bidirectional tendon actuation
      - PIP and DIP joints are fused
    - Digits 3 - 5 (flexion/extension), unidirectional tendon actuation via a compliant coupling (spring)
      - DIP joints are fused
  - Digits 1 and 2 have a series spring for extension but not for flexion
  - The bidirectional tendon configuration eliminate the need for parallel springs
  - The unidirectional tendon reduces the amount of spooled tendon by 2

- Each DOA is actuated by a Faulhaber 1226 brushless DC servomotor
  - 64:1 planetary gearhead
  - Custom two-way clutch unit
  - Bidirectional or unidirectional tendon pulley
  - See [10] and/or figure 3 for more detailed description of motor unit
- Results:
  - Thumb and pointer finger are each capable of 25 N
  - The combined efforts of digits 3 - 5 provide 16 N
  - Each finger has a max speed of 6 Hz
  - The hand is able to provide all grasps for which the authors intended
    - See figure 4



Figure 4

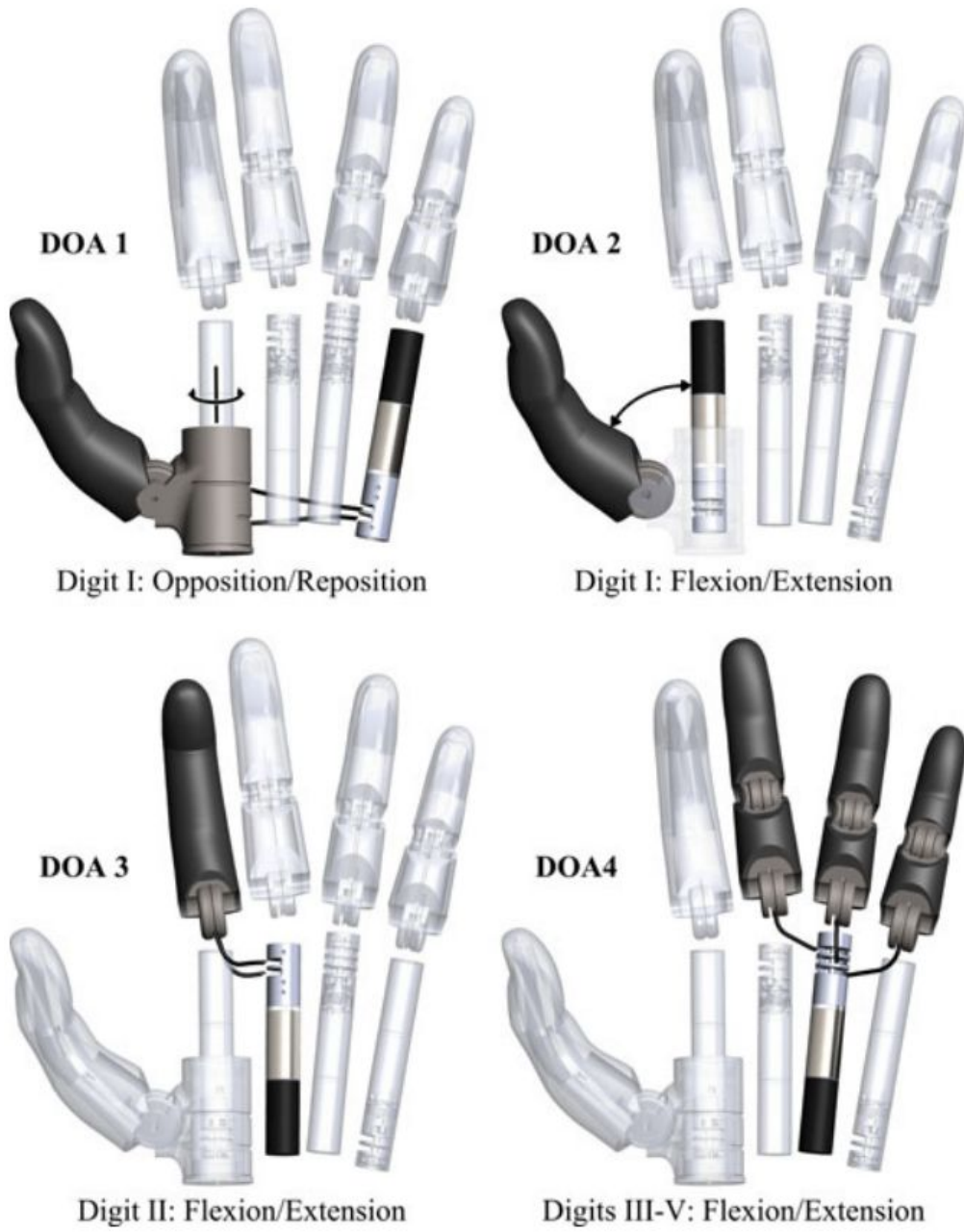


Figure 1

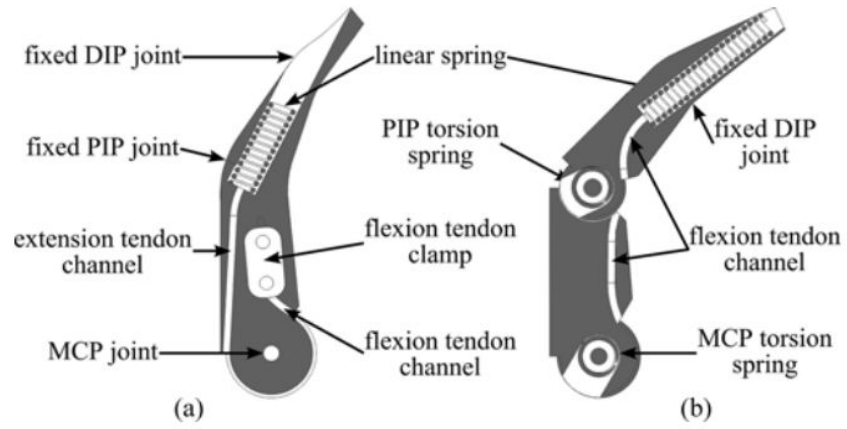


Figure 2

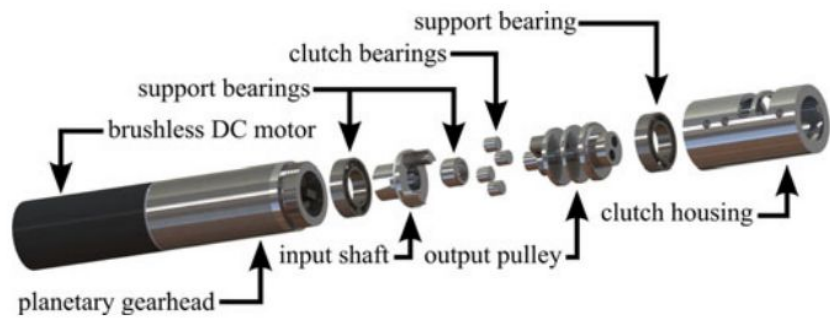


Figure 3

## Design of a multi grasp transradial prosthesis 2011

T. E. Wiste, S. A. Dalley, H. A. Varol, M. Goldfarb.

- Goal:
  - Present the design of a new intrinsically actuated prosthetic hand that can achieve eight grasp postures
    - Achieve force and speed characteristics appropriate for most activities of daily living
    - Adhere to appropriate size and weight constraints
- Background:
  - See background section of document 1 in this folder
- Related work:
  - Academic:
    - 15 DOF driven by a single ultrasonic motor through a 15-way differential coupling [1]
    - 9 DOF (3 fingers, 3 DOF per finger) driven by two actuators [2, 3]
      - One actuator controls all 6 joints in digits 2 and 3
      - One actuator controls all 3 joints in the thumb, using a Geneva wheel mechanism to switch control between two thumb movements based on input range
    - 16 DOF driven by four actuators [4, 5]
      - Two motors to actuate thumb
      - One motor to actuate index finger
      - One motor to actuate other three fingers through a compliant differential coupling
    - 16 DOF driven by six actuators [6] and [7] (11 DOF, similar motion)
      - One actuator per finger, two for the thumb
    - 8 DOF driven by five electrohydraulic valves [8, 9]
  - Commercial:
    - i-LIMB hand (Touch Bionics) and Bebionic hand (RSL Steeper)
      - 10 DOF (2 per finger) driven by five motors
    - Michelangelo hand (Otto Bock)
      - 6 DOF driven by two actuators
- Design objectives:
  - Achieve six grasp types (tip, lateral, tripod, cylindrical, spherical, hook)
  - Achieve point and platform postures
  - Provide fingertip forces and joint velocities commensurate with typical activities of daily life (ADLs)
  - Total hand mass less than 500g
- Implementation:
  - 16 DOF driven by four actuators (see **figure 1** and **figure 2**)
  - One motor each to actuate:
    - Thumb flexion (digit 1)

- Palmar abduction (digit 1)
- Index finger flexion (digit 2)
- Flexion of the remaining fingers (digits 3-5)
- Description of actuator units: (see **figure 4**)
  - Utilized a brushless motor (Faulhaber 1226B) and planetary gearhead (Faulhaber 12/4 64:1)
  - Two-way clutch to prevent backdriving the motor (see **figure 5**)
    - In forward drive, the input shaft drives the pulley through the clutch bearings
    - In back drive, the pulley wedges the clutch bearing against the output assembly housing, locking the system
- Description of structure: (see **figure 3**)
  - Power transmission:
    - Tendon-based to minimize mass and enhance compactness
    - Unidirectional tendon configuration for flexion, with extension being achieved using torsional springs embedded in each joint (see **table 1**)
  - Manufacturing:
    - Fabricated with stereolithography (SLA) process from a thermoplastic resin (WaterShed 11 120)
    - Strengthened with nickel coating (SLArmor process)
    - Integrated electrical wire routing in the palm and integrated tendon routing in the palm and all digits
- Sensing:
  - When the fingertip is not in contact with an object, the tendon force is a well-known function of tendon displacement
  - By measuring motor displacement vs. actuator current draw, one can ascertain when each finger has come into contact with an object
- Results:
  - The hand succeeded in achieving the desired grasps (see **figure 6**)
  - Index finger exerts up to 35 N in flexion, thumb exerts up to 30 N in flexion
  - Digits 3-5 collectively exert 15 N in flexion
  - The clutch mechanism prevented backdriving up to 790 mNm, which corresponds to a 630 N load in the test tendon
  - Hand weighs 320 g
  - For full hand specs, see **table 2**

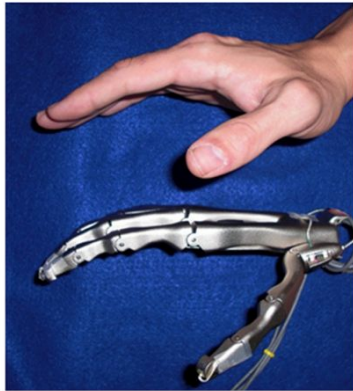
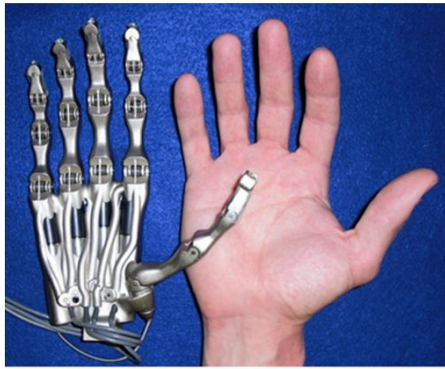


Fig. 1 Hand prosthesis prototype (without cosmesis), shown with intact hand for reference

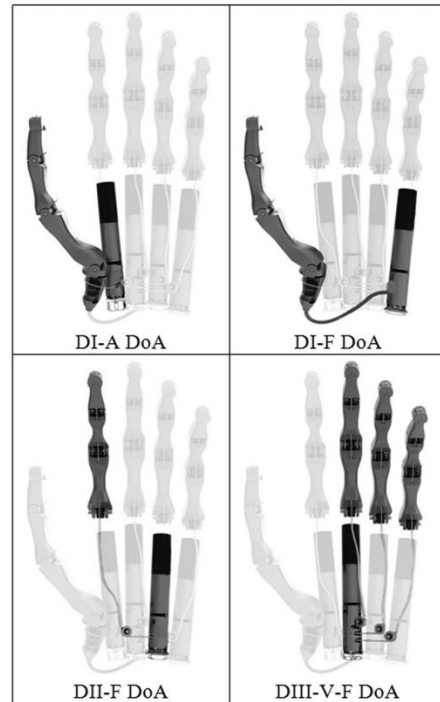


Fig. 2 Computer rendering of hand with palm structure removed, illustrating the motor unit layout and tendon routing for each respective degree-of-actuation (DoA). Note that the thumb flexion tendon exits through the dorsal aspect of the hand and is routed through a flexible cable housing (visible in the figure), while all other tendons are routing via pulleys and channels in the palm structure.

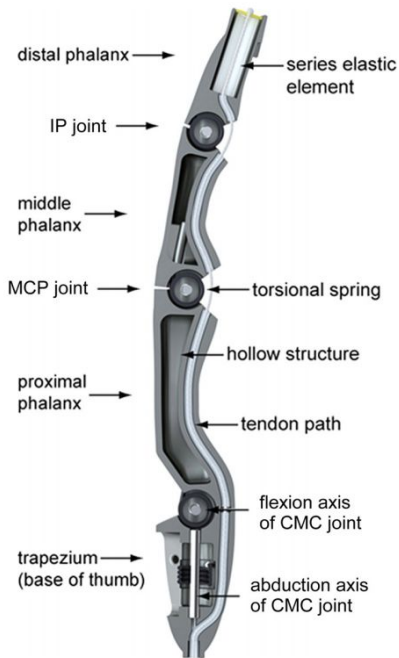


Fig. 3 Section view of thumb, showing tendon routing, torsional springs (in each joint), and series elastic elements (in distal phalanx)

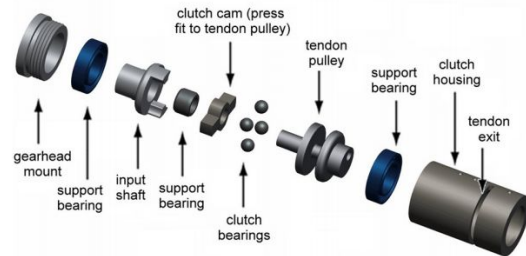


Fig. 4 Exploded view of a motor unit output assembly, showing integrated two-way clutch and tendon pulley

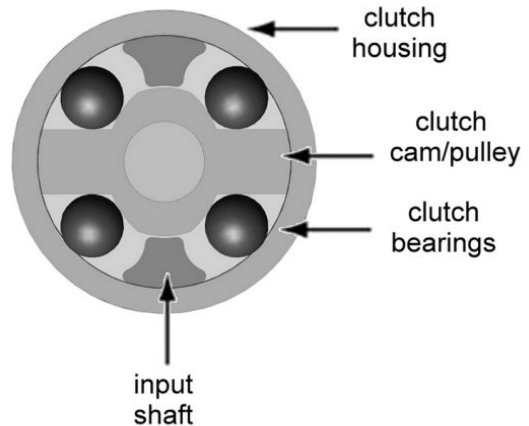


Fig. 5 Sectional view through two-way clutch

**Table 1 Range of motion and torsional spring stiffness in each joint**

| Joint                       | Range of Motion (Deg) | Torsional Spring Stiffness (N-mm/deg) |
|-----------------------------|-----------------------|---------------------------------------|
| Thumb CMC (abduction)       | 90                    | 0.80                                  |
| Thumb CMC (flexion) and MCP | 105                   | 0.85                                  |
| Index MCP and PIP           | 105                   | 0.85                                  |
| Thumb IP, Index DIP         | 85                    | 1.50                                  |
| DIII-V MCP and PIP          | 105                   | 0.63                                  |
| DIII-V DIP                  | 85                    | 1.00                                  |

**Table 2 Summary of prosthetic hand technical specifications**

| Specification  | VU Hand |
|--|---------|
| Degrees of freedom                                   | 16      |
| Number of actuators                                  | 4       |
| Mass (w/o cosmesis, battery, electronics)            | 320 g   |
| Grasp patterns                                       | 8       |
| Grasp speed (time to close)                          | 280 ms  |
| Audible noise (dBA at 1 m)                           | 52.1    |
| Max index fingertip force (70% excursion)            | 22 N    |
| Max index thumb tip flexion force (70% excursion)    | 19 N    |
| Max DIII-V combined fingertip force (70% excursion)  | 10 N    |
| Max thumbtip abduction force (70% excursion)         | 4.5 N   |
| Max index fingertip force (100% excursion)           | 34 N    |
| Max index thumb tip flexion force (100% excursion)   | 29 N    |
| Max DIII-V combined fingertip force (100% excursion) | 14 N    |
| Max thumbtip abduction force (100% excursion)        | 7 N     |

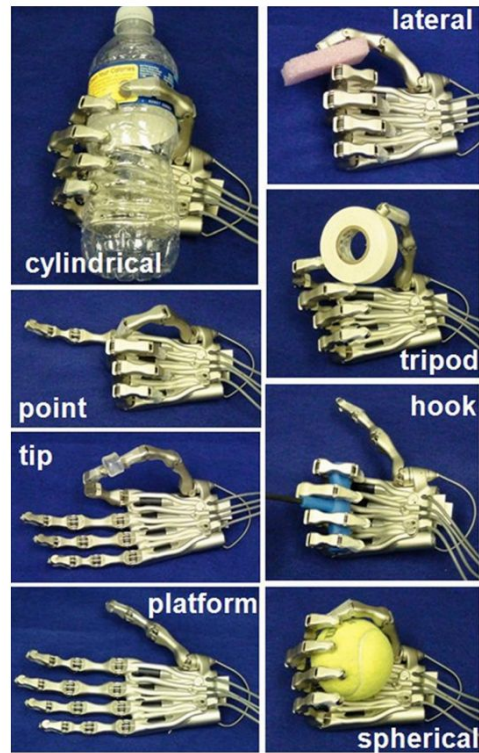


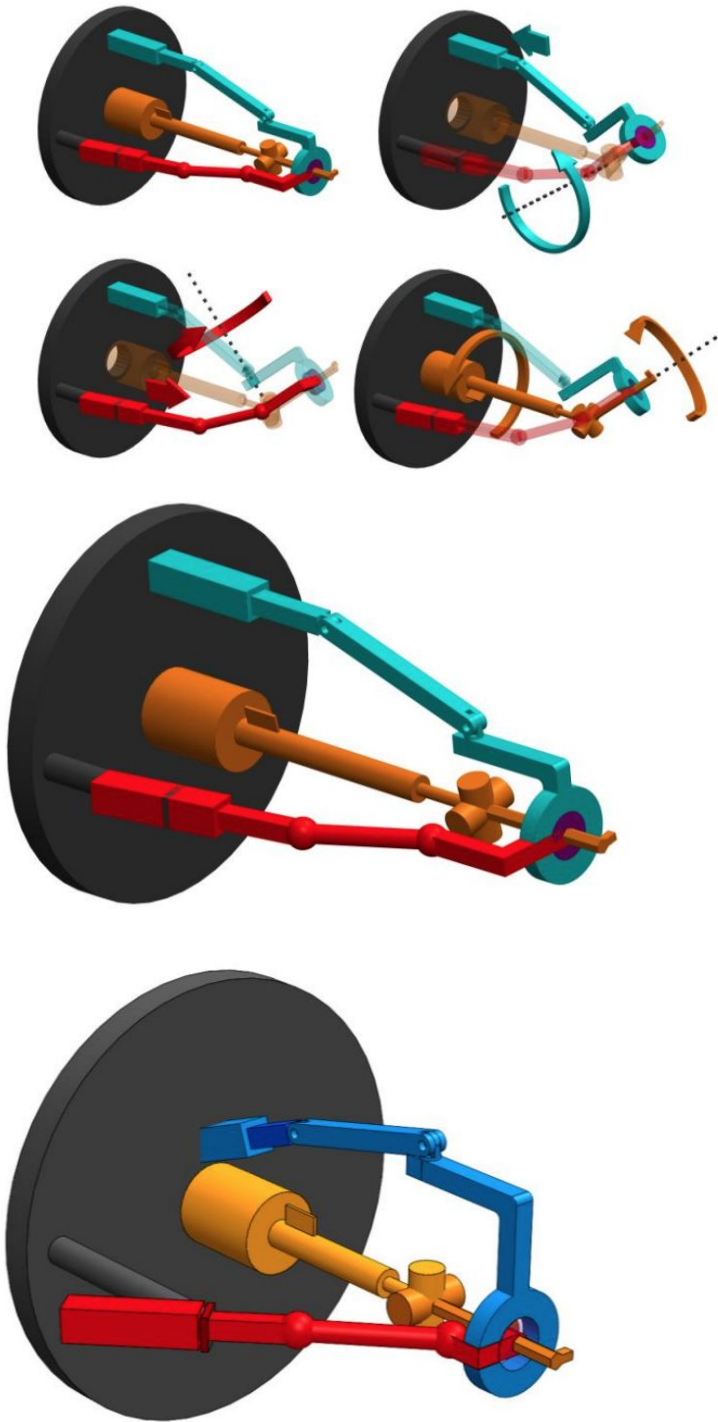
**Fig. 6 Six hand grasps and two hand postures, which constitute one of the primary design objectives of the hand prototype**

# Wrist mechanisms

## Kinematic optimization of a novel partially decoupled three degree of freedom hybrid wrist mechanism 2018

Neil M. Bajaj and Aaron M. Dollar.

- Goal:
  - Create a 3-DOF hybrid wrist mechanism that avoids long serial chains and the complexity of coupled parallel systems
- Terminology:
  - Serial chain:
    - Motors attached one after the other
    - Advantage is that one DOF is actuated by only one motor, and doesn't affect the positions of the other motors
      - Easy to control
    - Disadvantage is that by putting motors one after the other, the whole assembly becomes really long
  - Parallel system:
    - Motors placed side by side, but with the outputs coupled in some way to produce multi-DOF movement
    - Advantage is that the system can be made very compact
    - Disadvantage is that, since the output shafts are coupled, moving one actuator generally moves another
      - Difficult to control
    - Examples:
      - *Agile eye*
  - Hybrid system:
    - Combination of serial and parallel mechanisms
    - Can be fully coupled, partially decoupled, or fully decoupled
    - Advantage is that a hybrid mechanism can have a higher stiffness and bandwidth than a comparable serial or parallel mechanism
    - Disadvantage is that they are harder to design
- Implementation:
  - 2-DOF parallel pointing mechanism
  - 1-DOF serial mechanism to actuate roll (twisting of the wrist)
- Benefits:
  - Partial decoupling allows for optimization of each DOF's speed and torque requirements individually
- Mechanism:



# Lower-limb mechanisms

## Biomechanical considerations in the design of lower limb exoskeletons 2011

Massimo Cenciarini and Aaron M. Dollar.

- Goal:
  - Summarize the current state of the science that lies behind the design of exoskeletons
- See **figure 1** for complete overview
- Kinematic considerations:
  - The mechanics of the exoskeleton should comply with that of the limb and therefore not interfere with its natural motion [1, 21]
  - Provide torques at joints that are compatible with those of the human body
  - Challenges:
    - Non-ideal mechanics of certain joints [21]
    - The mechanics of gait change substantially between people
- Degrees of freedom:
  - Hip:
    - Three rotational DOFs, considered a ball-and-socket joint [19]
    - Flexion/extension is the primary DOF used in locomotion [21]
    - Adduction/abduction
    - Internal/external rotation (along axis of leg)
  - Knee:
    - Two rotational DOFs, considered a condyloid joint [19]
    - Flexion/extension
    - Internal/external rotation (small, manifests itself in ankle rotation)
  - Ankle:
    - Two rotational joints, considered as a hinge joint primarily [19]
    - Flexion/extension is the main DOF with the largest range of motion
    - Adduction/abduction has a small range of motion
- Joint torques:
  - Clinical gait analysis (CGA) data sources are a good start for the initial design of the actuation [4]
  - Most designers use maximum values as requirements for the sizing of their actuators
- Considerations on other design factors:
  - A device is considered anthropomorphic when the elements constituting the exoskeleton frame are sized following the proportions of the human body
  - The “end-point based” approach is not fully anthropomorphic, but rather makes sure the end-point of the exoskeleton matches the end-point of the limb

| Bio-mechanical Properties | Joints | Values for Biological Lower Limb [1, 17-19]  | Augmenting Exos  |                                  |                                |  | Assistive Exos                             |  |                                  |                               |
|---------------------------|--------|--|--|----------------------------------|--------------------------------|--|--|--|----------------------------------|-------------------------------|
|                           |        |  | BLEEX (Univ. of California) [4, 20, 21]  | MIT Exoskeleton (MIT) [2, 5, 22] | MIT Knee Exoskeleton (MIT) [9] | NTU-LEE (Nanyang Technological Univ.) [10] | DGO/Lokomat (Hocoma, Switzerland) [11, 23] | LOPES (Univ. of Twente) [12, 24, 25]                   | KNEXO (Brussels University) [13] | ALEX (Univ. of Delaware) [14] |
| DOF                       | Hip    | 3  | 3  | 3                                | N/A                            | 2  | 1  | 2  | 1 (un-actuated)                  | 2                             |
|                           | Knee   | 2  | 1  | 1                                | 1                              | 1  | 1  | 1  | 1                                | 1                             |
|                           | Ankle  | 1 (+1) <sup>a</sup>  | 3  | 2                                | N/A                            | 2  | N/A  | N/A  | N/A                              | 1                             |
| ROM [deg]                 | Hip    | 140/15 (F/E) <sup>b</sup> ; 40/30-35 (Ad/Abd) <sup>c</sup> ; 15-30/60 (Int/Ext) <sup>d</sup> | 121/10 (F/E) <sup>b</sup> ; 16/16 (Ad/Abd) <sup>c</sup> ; 35/35 (Int/Ext) <sup>d</sup> | 45/20 (F/E) <sup>a</sup>         | N/A                            | 60/20 (F/E) <sup>b</sup>                   | N/A  | 60/30 (F/E) <sup>b</sup> ; 15/15 (Ad/Abd) <sup>c</sup> | N/A                              | N/A                           |
|                           | Knee   | 120-140/0-10 (F/E) <sup>b</sup> ; 10-15/30-50 (Int/Ext) <sup>d</sup>                         | 121/0  | 90/0                             | 100/0                          | 120/0                                      | N/A  | 90/0   | 90/0                             | N/A                           |
|                           | Ankle  | 40-50/20 (F/E) <sup>b</sup> ; 30-35/15-20 (Inv/Ev) <sup>a</sup>                              | 45/45 (F/E) <sup>b</sup> ; 20/20 (Inv/Ev) <sup>a</sup>                                 | 15/15 (F/E) <sup>a</sup>         | N/A                            | 30/20 (F/E) <sup>b</sup>                   | N/A  | N/A  | N/A                              | N/A                           |
| Torque [Nm]               | Hip    | 140/120 (F/E) <sup>b</sup> [Walking]<br>40-80 [Running]                                      | -150:120 (F/E) <sup>b</sup>  | 130                              | N/A                            | 118 (F/E) <sup>b</sup>                     | 50 (280 max) (F/E) <sup>b</sup>            | 65 (F/E) <sup>b</sup> ; 30 (Ad/Abd) <sup>c</sup>       | N/A                              | 100 (F/E) <sup>b</sup>        |
|                           | Knee   | 50/140 [Walking]<br>125-273 [Running]  | -100:120   | 50                               | ~135                           | 118 (F/E) <sup>b</sup>                     | 30 (160 max) (F/E) <sup>b</sup>            | 65   | 70                               | 100 (F/E) <sup>b</sup>        |
|                           | Ankle  | 165 (E) <sup>b</sup> [Walking]<br>180-240 [Running]  | -200:150 (F/E) <sup>b</sup>  | 90                               | N/A                            | 118 (F/E) <sup>b</sup>                     | N/A  | N/A  | N/A                              | N/A                           |
| Velocity [rad/s]          | Hip    | N/A  | N/A  | 4                                | N/A                            | N/A  | N/A  | 1 (Ad/Abd) <sup>c</sup> ; 2 (F/E) <sup>b</sup>         | N/A                              | N/A                           |
|                           | Knee   | N/A  | N/A  | N/A                              | N/A                            | 10.5 (F/E) <sup>a</sup>                    | N/A  | 5 (F/E) <sup>b</sup>                                   | 10 (F/E) <sup>b</sup>            | N/A                           |
|                           | Ankle  | N/A  | N/A  | N/A                              | N/A                            | N/A  | N/A  | N/A  | N/A                              | N/A                           |
| Frequency [Hz]            | Hip    | N/A  | N/A  | N/A                              | N/A                            | N/A  | ≥1   | 4 (full force range); 12 (small forces)                | N/A                              | N/A                           |
|                           | Knee   | N/A  | N/A  | N/A                              | N/A                            | N/A  | ≥1   | 4 (full force range); 12 (small forces)                | 3.5-4.5                          | N/A                           |
|                           | Ankle  | N/A  | N/A  | N/A                              | N/A                            | N/A  | N/A  | N/A  | N/A                              | N/A                           |

a. The foot has 3 DOF and is characterized by Inversion/Eversion

b. Flexion/Extension

c. Adduction/Abduction

d. Internal/External

Figure 1

## Passive-dynamic leg design for agile robots 2015

A. Abate, R. L. Hatton, J. Hurst.

- Note:
  - Article is difficult to summarize and reading this summary won't truly compare to just reading the article. The math presented in the article is a little tricky but it's fairly easy to follow, and contains a lot of important concepts.
- Goal:
  - Leverage the familiar concepts of the jacobian, compliance, and inertia matrices to answer some difficult design questions:
    - Where do we place springs for spring-mass dynamics?
    - Which linkage shapes minimize touchdown impacts?
    - Where do we place motors for optimal energy use?
- Background:
  - Morphology and materials of limbs can enable efficient and immediate feedback control and stabilization *at the hardware level* [4]
  - Very high bandwidth, high power actuators, such as those in Boston Dynamics' hydraulic machines, are sometimes capable of overcoming unfavorable passive dynamics and exhibiting highly dynamic behavior, but they do so at the cost of extremely high power requirements
  - The SLIP model is difficult to physically implement
    - Several robots are based on the SLIP model though [12-16]
- Working example (to be referenced throughout the article):
  - 2-link, planar mechanism (see **figure 3**)
  - Kinematic (physical) model is decomposed into a virtual (SLIP) model
    - The jacobian matrix  $J$  transforms between kinematic coordinates (joint space) and virtual coordinates (task space)
      - Useful because it's easier to model forces in task space
      - Basis of task space are the leg length and leg angle
      - Basis of joint space are the two joint angles
    - Any individual joint position is a function of all motor angles and all spring deflections (linear combination of the two so that motor and spring placement can be handled separately)
  - Joint space positions are determined by motor angles and spring deflections according to  $\theta = G_m\varphi + G_s\delta$ 
    - $\theta$  (joint angles),  $\varphi$  (motor angles),  $\delta$  (spring deflections) are vectors
    - $G_m$  and  $G_s$  are matrices (or rank 2 tensors)
- Impact inertia analysis:
  - Impacts remove valuable energy from heavy, unsprung systems
  - Relevant mathematical objects:
    - Joint space inertia matrix ( $m$ )
      - Relates joint space accelerations  $\partial_t^2\theta^u$  to joint space torques  $\tau^u$

- Leg (task space) acceleration is  $\partial_t^2 L_v \approx J_{\mu\nu} \partial_t^2 \theta^\mu$  (eq. 10)
- Activity matrix (M)
  - Relates task space accelerations  $\partial_t^2 L$  to task space forces  $F$
  - Defined as  $J m^{-1} J^T$ , which we recognize as the coordinate transformation of a rank two tensor  $(M^{\mu\nu})^{-1} = J^\mu_\alpha J^\nu_\beta (m^{\alpha\beta})^{-1}$
  - Can be represented as an ellipse, where the inverse of the lengths of the major and minor axes represent the “intensity” of the resulting impact from a force along that axis (see **figure 4**)
- Compliance analysis:
  - The idea of passive-dynamic design is to have the hardware generate desired behaviors so that the control system doesn’t have to enforce them
    - In our case, the desired behavior is that leg length forces result in leg length deflections
    - Axial leg forces shouldn’t create off-axis deflections, which destabilize the robot and require controller intervention
  - Relevant mathematical objects:
    - Compliance matrix  $C$ 
      - Relates infinitesimal leg deflections to infinitesimal task space forces:  $C dF = dL$ 
        - Where  $C(\theta) = J G_s c G_s^T J^T$
        - And  $c = \frac{d\delta}{df}$ , the spring compliance matrix
          - $\delta$  is the spring deflection vector and  $f$  is the force vector (locally applied to each spring)
          - Diagonal if the springs do not interact
      - To exhibit desired behavior (leg forces generate *only* leg deflections), two things must be true:
        - $C$  is symmetric
        - $C$  is diagonal (proof in eq. 17 - 24)
      - Can be represented as an ellipse centered at the toe, where the two axes should align with the length basis vector and the angle basis vector, with the magnitude of the axes representing the amount of deflection under a unit force (see **figure 6**)
- Motor placement:
  - “Geometric” work refers to energy lost from motors working against each other
    - Two-fold cost:
      - Cost from generating the excess work
      - Cost of reducing that excess energy to heat
  - One way to guarantee no geometric work is to have a one-to-one correspondence between motors and basis vectors (i.e. one motor controls one basis vector of movement)
    - Maximal manipulability occurs if motor basis vectors are orthogonal [21]

- This means that motor basis vectors should be completely aligned with the leg coordinate system
- Relevant mathematical objects:
  - The motor gearing matrix  $G_m$ 
    - To guarantee decoupled motor efforts, it must be the case that  $J G_m \equiv \text{diag}(a, b)$  (eq. 30)
- If a geometric work loop is discovered in the operation of a finalized mechanism, it may not be possible to remove it after the fact
- Future work:
  - Instead of using local matrices (which can only handle infinitesimal displacements), derive a tensor potential field surrounding each toe
    - This is an extension of the compliance ellipse into large deflections, where the gradient of the potential field gives the combined spring force in task space
  - Coriolis forces will occur during leg swing, and careful design could couple knee flexion to aid leg recirculation as it does in forward-knee animals
  - Gravitational forces on the leg will also contribute to both starting and stopping the swing leg
    - Creates passive swing leg retraction behavior before touchdown, which has been shown to be stabilizing

## Design of a quasi-passive knee exoskeleton to assist running 2008

A. M. Dollar, H. Herr.

- Goal:
  - Present the design of a quasi-passive device that stores and releases energy in a spring that is actively placed/removed from being in parallel with the knee
- Related work:
  - RoboKnee
    - Simple exoskeleton for adding power at the knee joint
    - Consists of a linear series-elastic actuator connected to the upper and lower portions of a knee brace
- Biomechanics of running:
  - Human gait cycle is shown in **figure 2**
    - There are two aerial periods, each last 11% of the gait cycle
    - Walking and running are differentiated by having periods of double support (both feet on the ground) or double float (both feet in the air)
    - Running and sprinting are differentiated by the heel striking first or the toe striking first, respectively
  - Typical behavior of the knee during normal, level-ground running at 3.2 m/s for an 85 kg person is shown in **figure 4**
  - Energy cost per unit distance as a function of speed for walking and running is shown in **figure 5**
    - Max efficiency occurs at 1.1-1.4 m/s (walking)
    - Running at any speed requires 25% more energy than walking at that speed
- Working principle:
  - The parallel spring is applied conditionally, depending on the phase of the gait
    - At 3% (during the absorption phase), the spring is compressed as the knee flexes
      - Spring provides negative work to slow down knee that muscles would otherwise need to provide
    - At 14% (power generation phase), the knee begins to extend and the spring gives energy back
    - At 22%, the spring has fully extended and is detached for the remainder of swing phase
  - The current design could save the knee 19% of positive mechanical energy and 11% of negative mechanical energy (both per unit distance)
- Implementation:
  - Schematic diagram shown in **figure 7**, full CAD shown in **figure 8**, physical device shown in **figure 10**
  - Essentially, the spring can be moved up and down along a threaded rod, bringing it in/out of contact with a sliding joint that is connected on either end to the upper and lower portions of a knee brace

- Hardware specifications:
  - 60W brushed DC motor (RE 30, Maxon Motor)
  - 110 kN/m spring (actually two springs, each of stiffness ~55 kN/m)
  - Carbon fiber tubing
  - Rulon sliding bearings
  - Custom fabricated knee brace, based on joint kit (Townsend Design)
- Control:
  - Exoskeleton is controlled by estimating the gait phase and knee angle using optical encoder on the motor and a rotary potentiometer on the joint of the knee brace
  - Ground contact is detected using a switch in the sole of the user's shoe
- Results:
  - No relevant results (only bench tests of the device were done, no tests with users, for some reason)

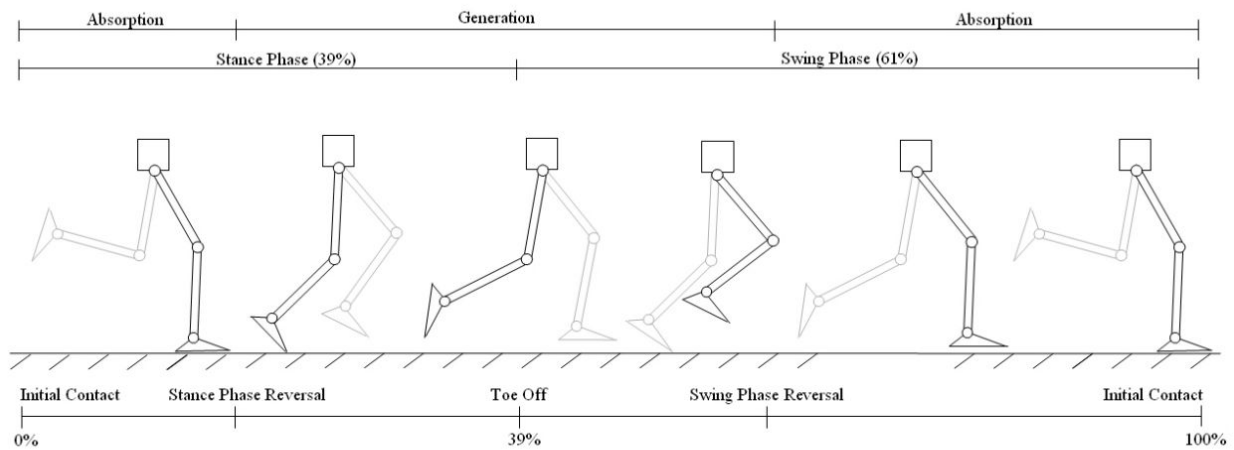


Fig. 2. Human running gait through one cycle, beginning and ending at heel strike (initial contact). Percentages showing contact events are given at their approximate location in the cycle. Adapted from [18].

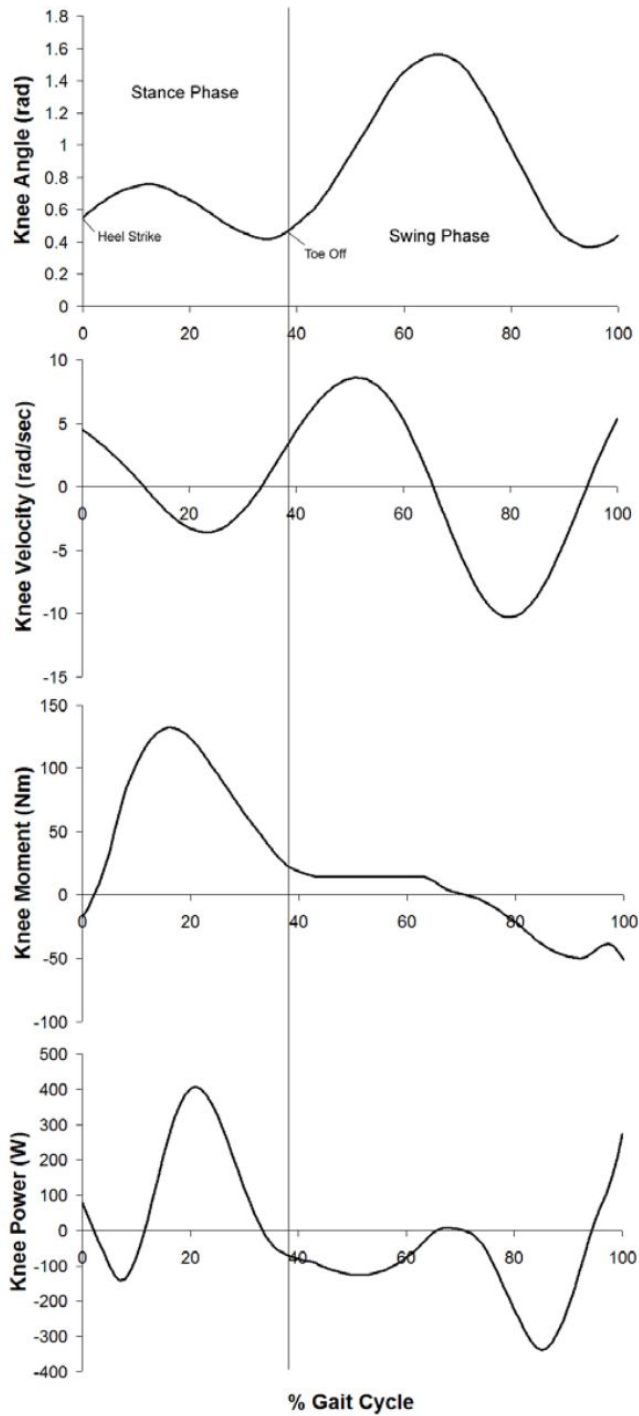


Fig. 4. Biomechanics of the knee of an 85kg individual running at 3.2 m/s showing knee joint angle, velocity, moment, and power (adapted from [18]).

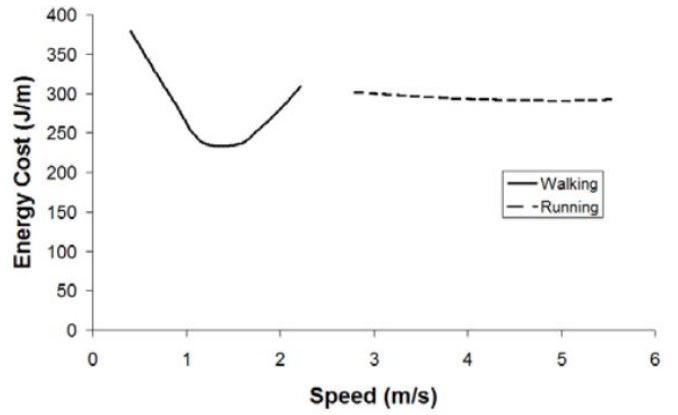


Fig. 5. Energy cost per unit distance as a function of speed for walking and running (adapted from [21]).

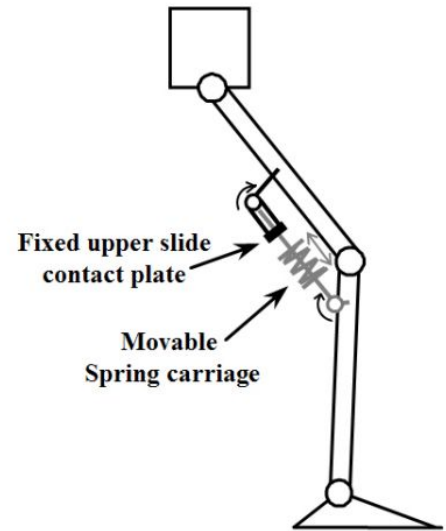


Fig. 7. Representative diagram of the running knee exoskeleton concept.



Fig. 8. CAD model of the actuator module.

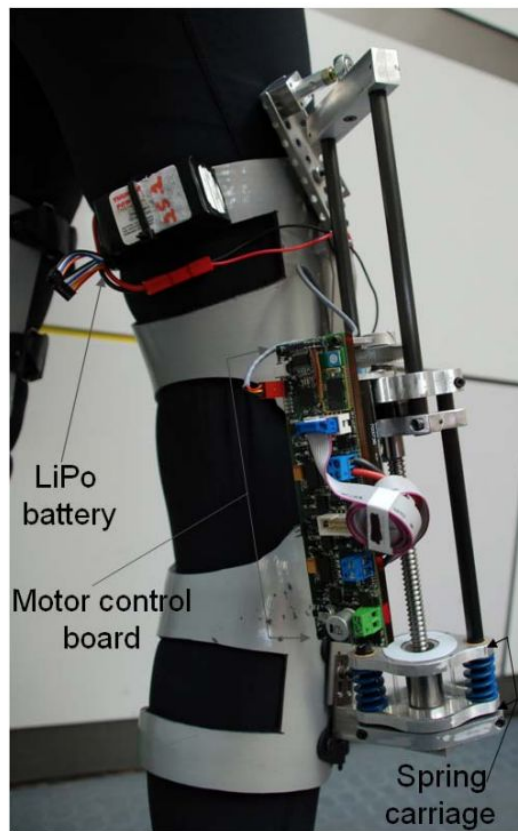


Fig. 10. Battery and control hardware.

# Walking theory

## Compliant leg behavior explains basic dynamics of walking and running 2006

H. Geyer, A. Seyfarth, R. Blickhan.

- Goal:
  - Argue that compliant legs (springy as opposed to stiff) are fundamental to the walking gait
  - Introduce the bipedal spring-mass model, which adds a second leg to the known running model and represents the simplest walking model using compliant legs
  - Look for stable locomotion of this model
- Background:
  - The inverted pendulum model for walking and the spring-mass model for running have developed into the conceptual basis for our understanding of legged locomotion
  - The ground reaction force (GRF) of walking is characteristically M-shaped
    - The inverted pendulum model cannot reproduce this (see figure 1)
  - There are more complicated models that can describe the dynamics of walking, but they are too complex to serve as conceptual models
- The bipedal spring-mass model:
  - Point mass at the COM, legs are two massless, linear springs of equal rest length and stiffness
  - The springs act independently and influence the dynamics only while in contact with the ground
    - I.e. the inertia of the airborne leg swinging through the air isn't accounted for by this model
  - Description of locomotion (see figure 2):
    - Model starts at an apex with the left spring in single support and the right spring in swing
    - Initially, the gravitational force exceeds the opposing spring force, the left spring shortens while rotating forward the COM height decreases
    - When the right leg touches the ground, the model enters the double-support phase
    - The additional push of the right stance-spring reverses the vertical and decelerates the horizontal COM motion
    - Owing to sufficient momentum, the forward progression continues to extend the left spring until it reaches its rest length
    - The left spring leaves the ground and enters swing until the COM reaches the apex
- Walking solutions reproducing experimental data:
  - Found three characteristic steady-state solutions A-C (see figure 3) whose gait patterns resemble those found in humans
    - Used the return map of a single step to find all solutions
      - Essentially, this method simulates a single step phase
      - Aborts if the model:

- Turns backward
- Takes off in single support (goes airborne)
- Stumbles and falls down (COM apex lower at end of step than at the beginning)
- Promising characteristics:
  - The COM oscillates around its landing height in the vertical GRF
  - The bipedal spring-mass model describes the 180°-out-of-phase changes in the forward kinetic and the gravitational potential energies (third row of figure 3)
  - Solutions A-C have differences that reflect those observed in walking at different speeds
    - For slow walking, symmetric stance-phase patterns with small amplitudes are observed that compare to the patterns in C
    - For faster walking, patterns with larger amplitudes are observed that compare to the patterns in A or B
- Notes:
  - In the parameter space, there are distinct regions of stable solutions (volumes, if you will, since our parameter space is three dimensional)
    - See figure 4
    - Solutions corresponding to the same domain are physically similar, but have slightly different behaviors
    - Solutions from different domains are physically different (e.g. 3 GRF peaks instead of 2)
  - The second leg does two things:
    - Prevents the COM from falling during locomotion
    - Gradually increases and decreases the effective load that acts on the other spring leg in its early and late stance
      - This 'load sharing' allows a stance spring to start from its initial rest length, oscillate an arbitrary number of times (where the number of times determines which parameter domain the solution belongs to), and return to its rest length
- Walking solutions unknown from experiments:
  - For lower system energies or slower speeds, the model discovers new domains of parameters for stable locomotion
  - Towards small system energies, the number of force peaks increases with each new domain
- Discussion:
  - The bipedal spring-mass model produces walking and running behavior
  - The identified multi-peak patterns show that walking and running are just two out of the many stable solutions to legged locomotion

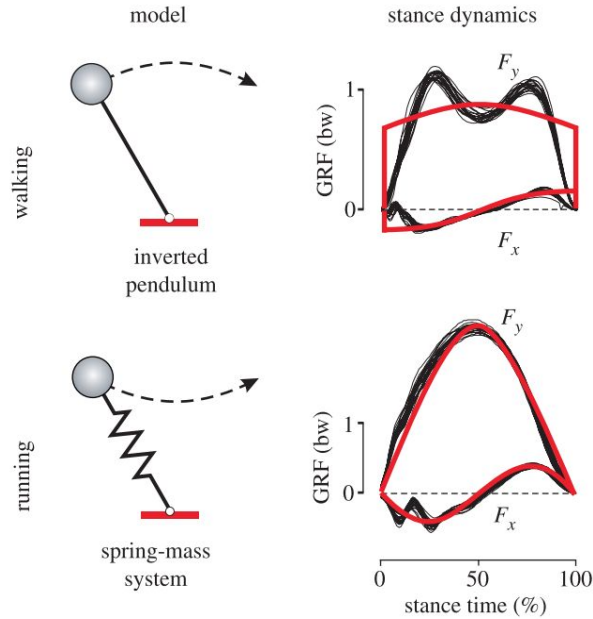


Figure 1. Standard conceptual models of legged locomotion and their predictive power with respect to walking and running dynamics. The inverted pendulum and the spring-mass system are the standard models for walking and running. The model-predicted stance dynamics (red lines) fit experimental data (black traces recorded from human treadmill walking at  $1.2 \text{ m s}^{-1}$  and running at  $4.0 \text{ m s}^{-1}$ ) only for the spring-mass model for running. Note that, in the inverted pendulum dynamics, delta functions appear at 0 and 100% stance time if one adds collision and push-off models imitating double support.  $F_{x,y}$ , horizontal and vertical ground reaction force (GRF) normalized to body weight (bw).

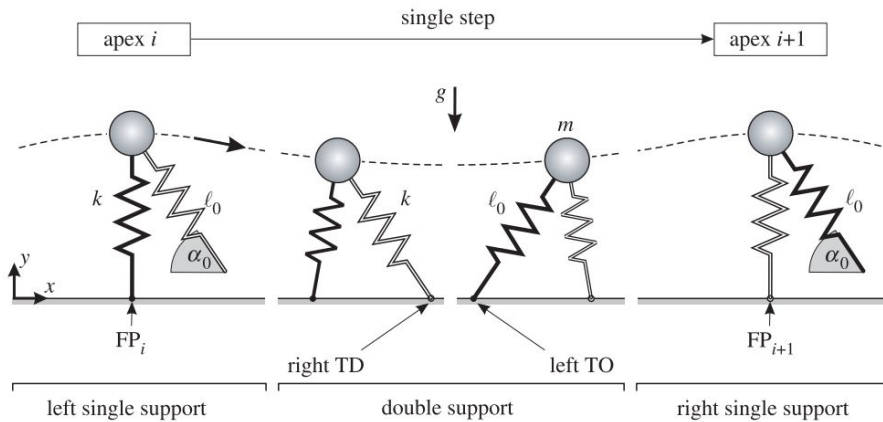


Figure 2. The bipedal spring-mass model. The model has two independent, massless spring legs attached to a point mass  $m$ . Both springs have stiffness  $k$ , rest length  $\ell_0$  and, in their swing phases, a constant orientation  $\alpha_0$  with respect to gravity ( $g$ , gravitational acceleration). A single step is shown that starts at the highest COM position in left leg single support (apex  $i$ ), includes the double support ranging from right leg touchdown (right TD) to left leg take-off (left TO), and ends at the next apex in right leg single support (apex  $i+1$ ). FP, foot point position in single support.

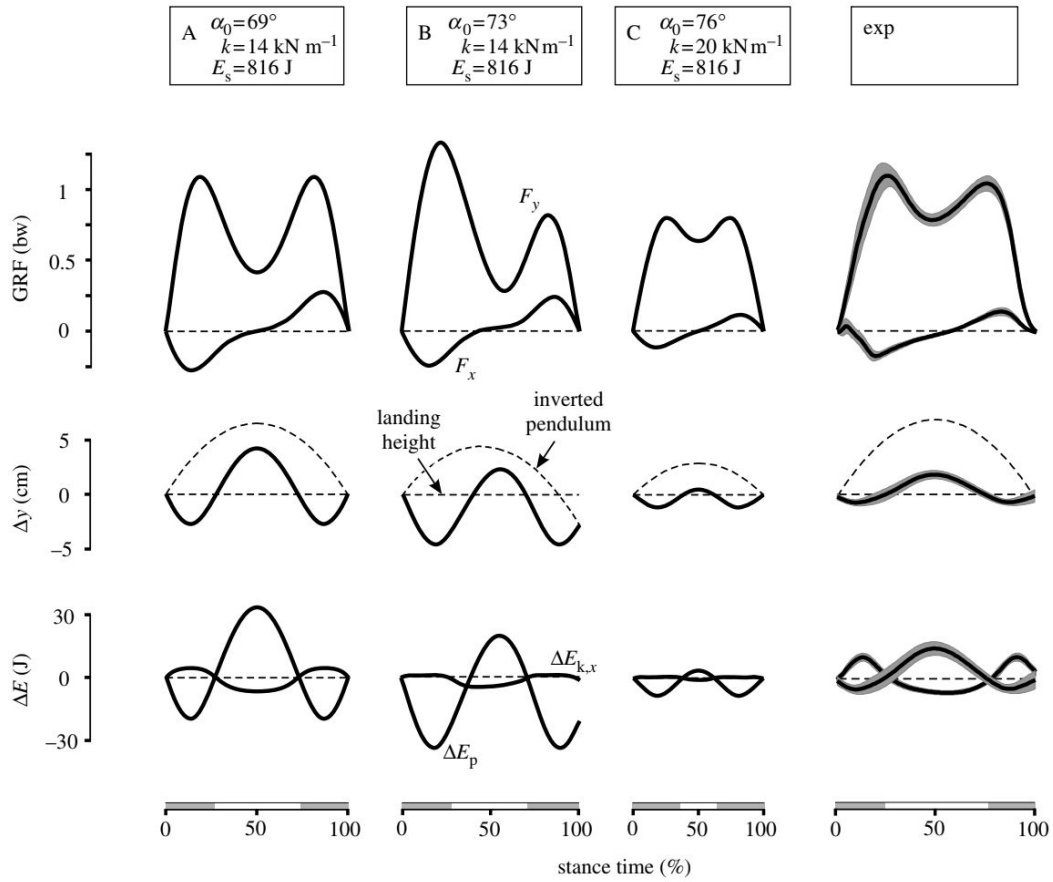


Figure 3. Stance-phase patterns of walking at about  $1.2 \text{ m s}^{-1}$ . (A–C) Examples of three characteristic steady-state solutions of the bipedal spring–mass model are compared with (exp) experimental results (mean and s.d. shown as line and shaded area) of five subjects (mean  $\pm$  s.d. of mass:  $81 \pm 3.5 \text{ kg}$ , leg length:  $1.07 \pm 0.03 \text{ m}$ ) walking on a treadmill (Adal3D, TecMachine, France; with force sensors recording horizontal and vertical GRFs). The subplots show horizontal and vertical GRFs,  $F_x$  and  $F_y$ ; vertical displacement,  $\Delta y$ ; and changes in forward kinetic and gravitational potential energies,  $\Delta E_{k,x}$  and  $\Delta E_p$ . The vertical displacement is compared with that of an inverted pendulum (dashed line). The shaded segments at the time-scales denote double supports. The depicted lengths of the time-scales reflect the absolute stance times.

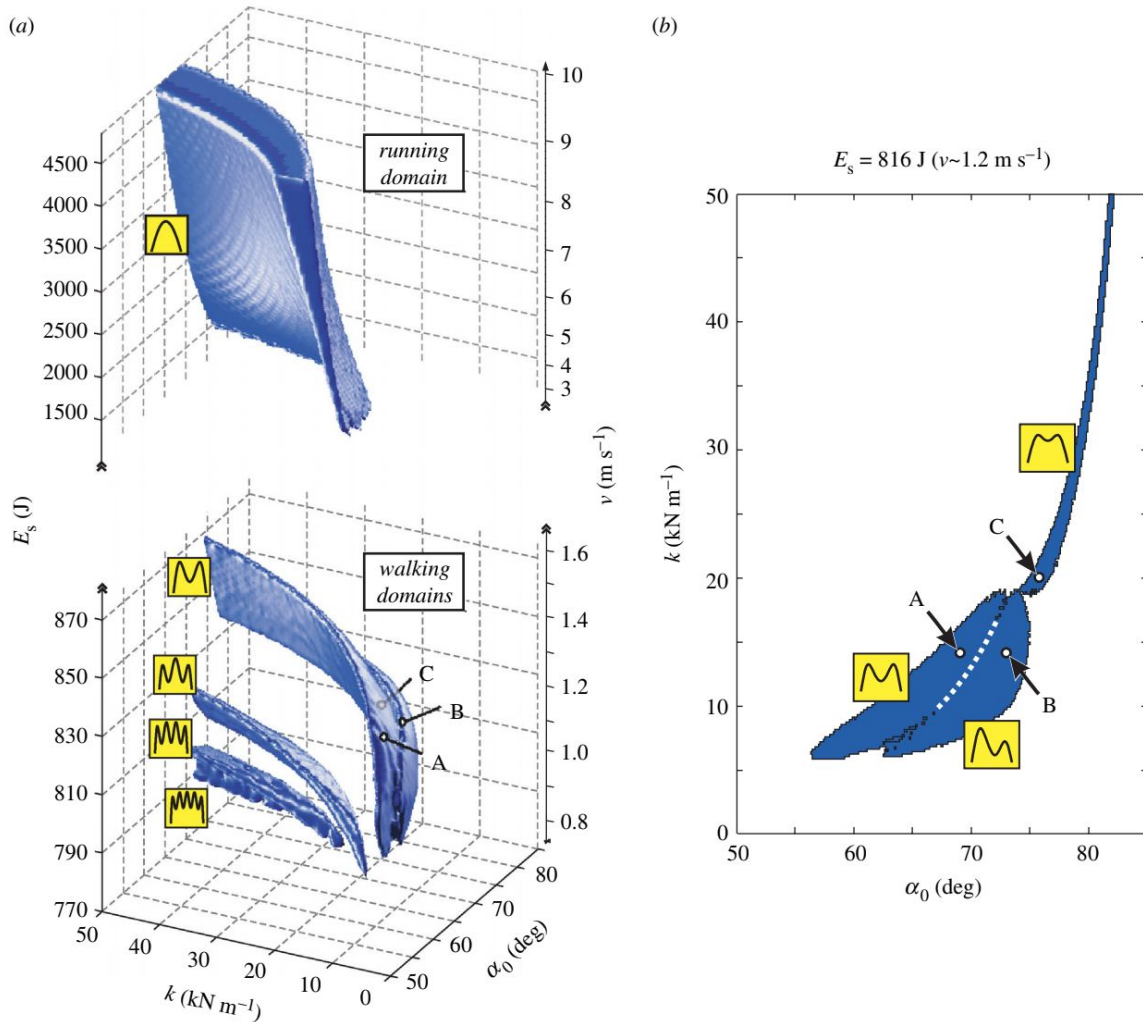


Figure 4. Parameter domains for stable walking and running. (a) Combinations of angle of attack  $\alpha_0$ , spring stiffness  $k$  and system energy  $E_s$  leading to stable locomotion are shown. Related to  $E_s$ , the locomotion speed  $v$  is shown, which is the average speed of all solutions that belong to one system energy (maximum deviation  $0.1 \text{ m s}^{-1}$  at  $E_s = 800 \text{ J}$ ). The model finds stable walking at low energies or slow speeds (walking domains): next to the domain with double-peak patterns of the vertical GRF, domains with multi-peak patterns exist (small icons). Owing to the limited scan resolution, only domains with up to five peaks are resolved, and the four- and five-peak domains seem to overlap. Circles indicate the parameter sets of the examples A–C shown in figure 3. In addition to walking, the model finds stable running with single-peak vertical GRF above an energy or speed gap of about  $500 \text{ J}$  or  $1.5 \text{ m s}^{-1}$  (running domain). Note the different scales of system energy at the walking domains and the running domain. (b) A slice at  $E_s = 816 \text{ J}$  ( $v \sim 1.2 \text{ m s}^{-1}$ ) through the walking domain with double-peak patterns is shown. Three sub-domains of parameters exist that lead to three qualitatively different steady-state patterns (small icons) exemplified by the three solutions A–C (compare figure 3).

# Walking control techniques

## Actuated dynamic walking in a seven-link biped robot 2010

David Braun, Jason Mitchell, Michael Goldfarb.

- Goal:
  - Design and construct a seven-link biped robot appropriate for implementation of the fully actuated, non-kinematic walking approach described in [19]<sup>1</sup>
- Design considerations:
  - To avoid suppression of the inertial dynamics of the biped, the robot was design with low-output impedance (backdrivable) joints
- Mechanical design:
  - 1.2 m tall, total mass of 14.3 kg
  - Upper body:
    - Carries 4.54 kg of weight distance 0.2 m from the hip joint to simulate a head, arms, and trunk
    - Has a single-axis accelerometer gyroscope (ADXR150) to measure angular velocity in the sagittal plane (forward-backward)
  - Actuation:
    - Each unit consists of a 150 W brushed DC motor (Maxon RE40) and a low gear ratio planetary reducer (Maxon GP42C)
    - Gear ratios 21:1, 12:1, 21:1 for the hip, knee, and ankle units, respectively
  - Sensing:
    - Six joint encoders (1 for each motor)
    - MEMS gyroscope mounted on the upper body (described above)
    - Force sensing resistors integrated into each foot (Interlink 402 FSR)
      - Four per foot, 2 under toe, 2 under heel
    - Reference positions for the encoders is established in a static initialization phase with two accelerometers (ADXL203) located on the upper body and the upper right leg
      - Detects alignment using the gravity vector
  - Foot:
    - Foot-plate is supplanted with silicon rubber pads with high frictional properties, good abrasive durability, and appropriate shock absorption
- Control tuning;
  - Parameters were initially tuned in a numerical simulation of the biped, and subsequently, iteratively tuned during experimental implementation to provide a stable, yet relaxed, gait cycle
- Results:
  - The robot walks with extended knee stance support
  - Such a motion style is recognized to be energetically beneficial compared to a usual bent knee robot walking, but is different from human walking [18]

---

<sup>1</sup> Paper (2) in the parent folder of this document

- The robot utilized a rolling foot double-support phase and a preemptive ankle push-off to propel itself forward
  - This is known to be utilized by humans
- The cost of transport was measured to be  $\sim 0.31$  (slightly higher than the theoretical prediction, but still lower than Honda's ASIMO)
- The non-kinematic walking approach demonstrated here appears more relaxed and natural than usual approaches that require accurate joint trajectory tracking (see accompanying video)

## A control approach for actuated dynamic walking in biped robots 2009

David Braun, Michael Goldfarb.

- Goal:
  - Create a control system that enables fully dynamic biped walking, which can provide a more efficient gait than trajectory-tracking approaches
- Terminology:
  - Zero-moment-point approach (ZMP)
    - Frequently used trajectory-tracking approach to biped walking
    - Results in stiff and unnatural-looking gait
    - Low locomotive efficiency
      - Position-level information is dictated by the controller, and thus, integration of the inertial dynamics is not an essential part of the motion
      - Reshaping the natural dynamics of the robot is energetically expensive
    - Humans, on the other hand, leverage the natural dynamics of their limbs when walking
  - Dynamic walker
    - A robot where the motion of the walker is not dictated substantially by the controller, but rather is influenced significantly by the gravitational and inertial characteristics of the system
      - Limb dynamics play a big role in determining the joint angle trajectories
      - Joints should be backdrivable so that inertia can take effect
  - Passive dynamic walker
    - No actuators, only uses gravitational energy to move itself (must go downhill)
  - Actuator-assisted dynamic walker
    - Uses a reduced set of actuators
    - Very high efficiency, but not as robust or fast as full actuation
  - Fully actuated dynamic walker
    - Actuates all relevant joints
- Approach:
  - Subject the robot to a set of state-dependent torques generated by low gain spring-damper couples
    - If not for the low gain, the actuators would have too much influence on the joint angle trajectories, making the walker non-dynamic
  - Relax assumptions regarding robot configuration
  - Develop a model-based solution to transform the state-dependant control torques to actuator torques
    - Utilize the *Gauss principle of least constraint* (basically the principle of least action)

- Simulation:
  - Control parameters were considered to be a robust set when the biped would, within a few steps, converge to a stable, natural-looking gait
  - This walker converged to a natural-looking gait within a few seconds for all simulations
  - The mechanical cost of transport (ct) is (mechanical energy) / (weight x distance traveled)
    - For this walker:  $ct = 0.19$
    - For honda asimo:  $ct = 1.6$
    - For cornell actuator-assisted walker:  $ct = 0.05$
- Future work:
  - Automate the parameter tuning process

# Walking robots

## Walking and running with passive compliance 2018

Christian Hubicki, Andy Abate, Patrick Clary.

- Overview:
  - Paper is a summary of the development of the Assume The Robot Is A Sphere (ATRIAS) robot, which began in 2015 or earlier
- Goal:
  - Describe the mechanics of ATRIAS and how the controller exploits the interplay between passive dynamics and actuation to achieve robust locomotion
- Background:
  - A promising approach to stable control is to relinquish some authority to purposeful passive dynamics
    - Either by adding mechanical compliance or removing actuators
  - An often-used model for walking and running is the spring-loaded inverted pendulum (SLIP) model
    - Point-mass body, massless point toe, massless spring connecting them
- Mechanical overview:
  - See figure 1
  - Carbon-fiber legs for minimum inertia connected by series springs to the concentrated mass at the hips
    - With series compliance, unforeseen effects are softened
    - Energy can be recycled from step to step and released at higher rates than the motor alone can deliver
  - Kinematically, ATRIAS has:
    - Two planar legs comprising a parallel mechanism
    - Two actuators co-located at the hip
    - Distal toe
  - Six actuators total:
    - Two legs, each with hip extension, knee extension, and hip abduction
  - Passive foot that simulates a point contact at the ground but restricts yaw rotation
- Electrical/software overview:
  - See figure 2 for description of electrical system
  - All control processing is done by an onboard computer
    - Executes control software on top of the Simulink Real-Time kernel
  - Commercial-off-the-shelf motor drivers (200 A for leg motors, 60 A for hip motors)
    - All drive brushless three-phase motors in current control mode
  - Sensing:
    - Uses only proprioceptive sensors
      - High-res absolute encoders at each internal DOF
      - Completely determine the configuration of the robot, save for its translation with respect to the world frame
    - Otherwise completely blind to the environment
  - 44.4 V, 10 Ah, 65C-discharge-rate LiPo battery pack

- Capable of 650 A peak discharge (yikes)
- Control overview:
  - Uses behaviors rather than high-DOF model-based control
  - Does not require any preplanning
    - The stability of the gait is not tied to the existence of disturbance models
  - Joint compliance relates forces to deflections
    - Allows open-loop trajectories to interact with unexpected or nontrivial contact states
  - Knowing that forces will be exerted exactly opposite to contact disturbances allows the creation of controllers that are *open-loop stable* with respect to changes in the environment
  - Primary control concepts:
    - Clock-based stepping
    - Velocity-based foot placement
    - Soft transitions between swing and stance
    - Torso balance
    - Energy injection against controlled damping
  - Controller is written as native MATLAB code
- Results:
  - Able to walk on nonrigid surfaces, such as grass, soft foam, and turf field
  - Can walk stably without significant sensitivity to surface dynamics
  - Specs:
    - Max speed of 2.5 m/s
    - Step over 15 cm tall obstacles
    - Walk up slope of 15°
  - Battery pack was drained after 30 minutes of continuous stepping
  - Total cost of transportation (TCOT) is defined as (total energy) / (weight x distance traveled)
    - ATRIAS TCOT = 1.3
    - ASIMO's TCOT = 3.2
    - Cornell Ranger TCOT = 0.19
    - ATRIAS MCOT (mechanical instead of total) = 0.96

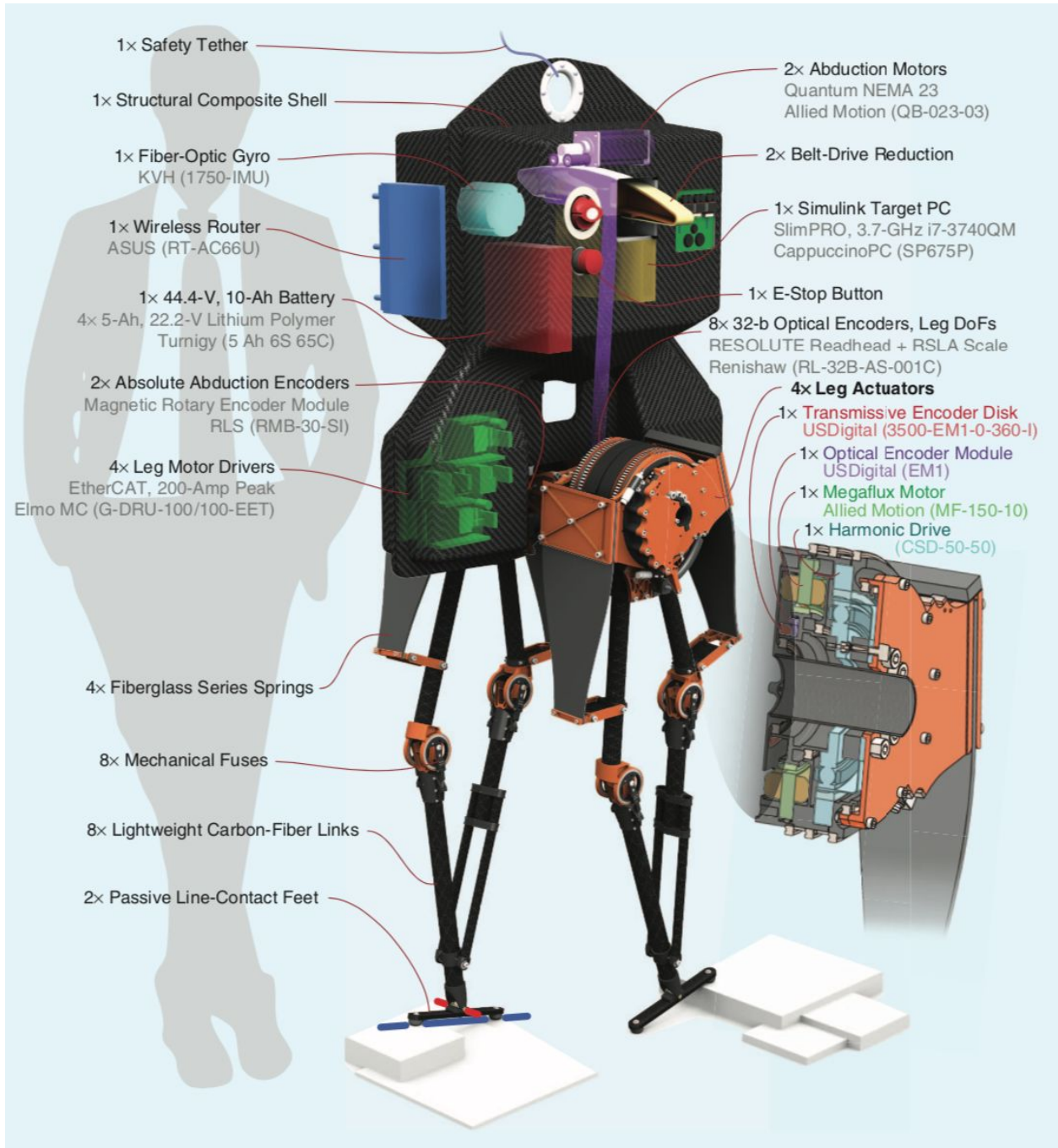


Figure 1

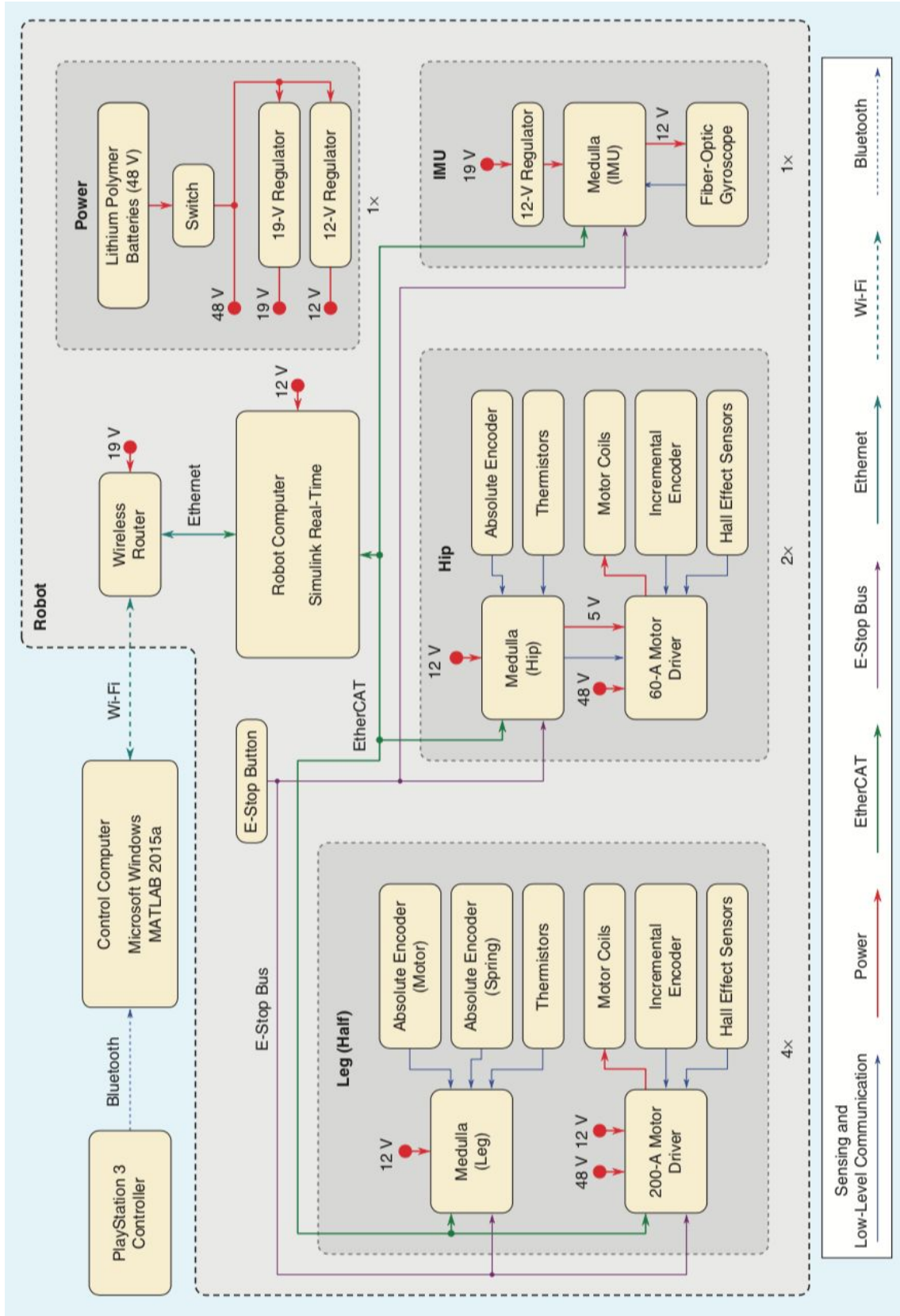


Figure 2

# Performance metrics

(coming soon)